

# Localization, morphology, and immunohistochemistry of spinal cord and dorsal root ganglion neurons that innervate the gastrocnemius and superficial digital flexor muscles in cattle

Roberto Chiocchetti, DVM, PhD; Annamaria Grandis, DVM, PhD; Cristiano Bombardi, DVM, PhD; Paolo Clavenzani, DVM; Alessandro Spadari, DVM; Arcangelo Gentile, DVM; Ruggero Bortolami, DVM

**Objective**—To determine the location, morphology, and neurochemical code of spinal cord and dorsal root ganglion neurons that innervate the gastrocnemius muscle (GM) and superficial digital flexor muscle (FDSM) in cattle.

**Animals**—5 healthy Friesian male calves.

**Procedure**—2 different types of neuronal retrograde fluorescent tracers (fast blue and diamidino yellow) were injected into the GM and FDSM, respectively. The neurochemical code (substance P, calcitonin gene-related peptide, galanin, and neuronal nuclear protein) of labeled neurons was investigated by immunohistochemistry.

**Results**—Neurons innervating the GM and FDSM were located along the L6-S2 spinal cord segments and ganglionic levels. A cranial-to-caudal topographic distribution for each muscle was found, indicating that the motor nuclei of the 2 muscles are organized by a somatotopic pattern. The GM and FDSM motoneurons were immunoreactive only for calcitonin gene-related peptide, whereas the afferent neurons were immunoreactive for all of the neurochemical markers considered.

**Conclusion and Clinical Relevance**—In our study, location and the extent of neurons that supply the GM and FDSM of cattle were characterized completely. Because the GM and FDSM are involved in spastic paresis of calves and it is thought that spastic paresis results from an excessive activity of the neuromuscular spindle reflex arc, findings in our study may be useful for further electrophysiologic and clinical studies. Knowledge of the neurochemical code of neurons that supply the GM and FDSM in healthy calves could be used to compare chemical alterations in the same neuronal population of affected calves. (*Am J Vet Res* 2005;66:710–720)

Many morphologic and electrophysiologic studies<sup>1-11</sup> have been performed on the cat and rat spinal cord motor and sensory neurons that inner-

vate the hind limb muscles, in particular the **gastrocnemius muscle (GM)**. At present, data are not available concerning the position, morphology, and neurochemistry of the bovine efferent and afferent neurons that innervate the GM and the **superficial digital flexor muscle (FDSM)** of the hind limb. The location of the neurons that innervate these muscles is of particular interest, as the GM and FDSM are directly involved in one of the most widespread diseases in cattle, inherited spastic paresis (also known as Elso Heel).<sup>12</sup> Inherited spastic paresis was initially described in 1922 in Europe<sup>3</sup> and is still a little understood disease of calves, the cause of which remains unknown. The pathogenesis of spastic paresis of calves may be closely related to subacute transmissible spongiform encephalopathies.<sup>13,14</sup> Inherited spastic paresis is a progressive condition of the GM and FDSM of calves that is characterized by hyperextension of the hock joint and accompanied by repeated spastic movements of the hind limb. Its pathogenesis, which is probably influenced by genetic factors, is not completely understood, but an overactive stretch reflex resulting from an upper motor neuron lesion may be the basis of spastic paresis.<sup>15</sup> Clinical signs of spastic paresis appear often in calves from 1 week to 12 months of age,<sup>16</sup> and both hind limbs can be affected. Inherited spastic paresis of calves may also involve other muscles of the hind limbs and forelimbs. Many types of treatment have been suggested, including tenectomy,<sup>b</sup> partial tibial neurectomy,<sup>17</sup> and triple tenectomy.<sup>18</sup> Some interesting results were obtained after the selective suppression of gamma efferent nerves by an epidural injection of a dilute procaine solution.<sup>19</sup> The selective resection (deafferentation) of the afferent nerves of the GM at the level of the dorsal spinal roots relieves or abolishes the clinical signs.<sup>15</sup>

The purpose of the study reported here was to determine the location, morphology, and neurochemical code of spinal cord and **dorsal root ganglion (DRG)** neurons that innervate the GM and FDSM in cattle. We used 2 different retrograde fluorescent tracers, **fast blue (FB)** and **diamidino yellow dihydrochloride (DY)**. The FB dye, which stains only the cytoplasm of neurons, was injected into the GM, whereas DY, which stains only neuronal nuclei, was infiltrated into the FDSM. To our knowledge, this is the first investigation coupling the morphology and

Received May 11, 2004.

Accepted June 23, 2004.

From the Department of Veterinary Morphophysiology and Animal Production (Chiocchetti, Grandis, Bombardi, Clavenzani, Bortolami) and the Veterinary Clinical Department (Spadari, Gentile), University of Bologna, 40064 Ozzano dell'Emilia, Bologna, Italy.

Supported by the Regione Emilia-Romagna grant.

The authors thank Dr. Giulia Bompadre Avoni for technical assistance.

Address correspondence to Dr. Chiocchetti.

the function of Rexed's lamina IX in the lumbosacral region of the spinal cord of cattle. Results of this research could be useful for studying other bovine neuronal diseases involving the lumbosacral region of the spinal cord and its afferent pathways, such as spastic syndrome (standing disease) of adult cattle<sup>20</sup> or bovine spinal muscular atrophy.<sup>21-24</sup>

We also investigated, by use of immunohistochemical procedures, **substance P (SP)**, **calcitonin gene-related peptide (CGRP)**, **galanin (GAL)**, and **neuronal nuclear protein (NeuN)** immunoreactivity of neurons. Because DRG neurons of horses and pigs have a partial cross-reactivity between SP and neurokinin A,<sup>25</sup> we thought it convenient to refer to the material detected with an antibody against SP as **tachykinin (TK)** immunoreactive throughout the text. Because we cannot rule out the possibility that the antibodies recognize substances other than the neurochemicals considered, the staining we observed should be considered SP-, CGRP-, GAL-, and NeuN-like immunoreactivity. For the sake of simplicity, however, we will use the terms immunoreactivity and immunoreactive. Preliminary results from part of this work have been reported.<sup>6</sup>

## Materials and Methods

**Animals**—Five male Friesian calves that were 67 to 90 kg in weight and between 2 to 4 months old were included in this study. Calves were maintained on a diet of hay and water ad libitum for 1 week before the experiment. The day before surgery, calves were kept without food. The University of Bologna Animal Experimentation Ethics Committee approved all procedures.

**Surgical procedures**—Calves were sedated with xylazine hydrochloride (0.04 mg/kg, IM). After 30 minutes, anesthesia was induced by IV administration of sodium thiopental (3 mg/kg) and maintained with a 1.5% to 2% (the dial setting on the vaporizer) isoflurane concentration delivered in an open circuit in 100% oxygen via a cuffed orotracheal tube. Subsequently, an orogastric tube was introduced to allow the emission of the continuous gas formed (to avoid ruminal meteorism). The surgical procedure was performed on the left hind limb with the calf in right lateral recumbency. The surgical field was prepared, and a skin incision of 25 to 30 cm in length was created in the visible groove between the biceps femoris and the semitendinosus muscles. Smooth dissection was performed between the 2 muscles (ie, through the caudal rim of the biceps femoris and the cranial rim of the semitendinosus muscle). Advancing in the cranial direction along the medial surface of the gluteobiceps muscle, the popliteal cavum was reached, in which the popliteal lymph node was detected as a landmark. The tibial nerve penetrates between the origins of the medial and lateral heads of the GM. The dorsal surface of the lateral head of the GM was smoothly dissected from the caudal surface of the belly of the FDSM. After the exposure of these structures was completed, the injection of fluorescent tracers was started. At the end of surgery, sutures were placed in a continuous pattern with 2-0 polyglycolide acid monofilament between the 2 previously divided muscular bellies; skin closure was performed with a simple interrupted suture with 2-0 nylon monofilament. Calves recovered from surgery and began to walk shortly after surgery and to eat hay on the first postoperative day.

**Injection of fluorescent tracers**—The exposed left hind limb muscles were slowly infiltrated with multiple-site injec-

tions of 2 fluorescent tracers, DY<sup>d</sup> (2% aqueous suspension) and FB(2% aqueous solution),<sup>e</sup> by use of 10- $\mu$ L Hamilton microsyringes. The DY produces a yellow fluorescence of the neuronal nucleus at an excitation wavelength of 360 nm, and FB produces a blue fluorescent labeling of the cytoplasm at the same excitation wavelength. Both the lateral and medial components of the GM received FB injections, and the FDSM was infiltrated with DY fluorescent tracer. Injections of FB into the GM were made where the tibial nerve penetrates the muscle and branches to supply the 2 parts of the muscle in the popliteal region. Different conditions were used for the infiltration of the FDSM. Because the lateral portion of the GM mostly covers the proximal head of this muscle, the FDSM was infiltrated along its length but it was not possible to see the nerves where fibers were reached. Each muscle was injected with a minimum of 400  $\mu$ L of fluorescent tracer. At least 40 injections of FB or DY were made in each muscle, and the aim of this operation was to infiltrate the major extension of the muscle surface. The syringe was gently withdrawn, and any tracer leakage was removed from the surface of the muscles.

**Distances and survival time**—The distances to be traveled by the dyes (the distance from the GM and FDSM to the DRG and spinal cord) were approximately 50 cm. To establish the optimal survival time for calves, we have considered the survival time used in a similar experiment performed on the rat GM<sup>26</sup> and also our own experience with these dyes in the visceral neural pathways in sheep.<sup>27</sup> For this study, a survival period of 5 weeks has been used.

**Tissue preparation**—At the end of the chosen survival time, calves were deeply anesthetized by use of sodium thiopental (15 mg/kg, IV) and euthanized by means of embutramide, mebenzonium iodide, and tetracaine hydrochloride administration. Following euthanasia, the T13-S5 spinal cord surrounded by the dural sack was immediately exposed in its full length through a dorsal laminectomy. In doing so, we did not cut the spinal roots to ensure the later exact identification of the different segments of the cord and the collection of the DRGs. After freeing the cord of the spinal dura, the spinal cord was divided in segments. Segmental boundaries were localized by means of the dorsal spinal roots and by counting them from the last thoracic spinal nerve, which is located just caudal to the 13th rib. The L5-S3 spinal cord segments and DRGs (ipsilateral and contralateral ganglia) were quickly removed from the vertebral canal, fixed in a flat vessel for 48 hours in 4% paraformaldehyde in phosphate buffer solution (0.1M; pH, 7.2) at 4°C, rinsed overnight in PBS solution (0.15M NaCl in 0.01M sodium phosphate buffer; pH, 7.2) and stored at 4°C in PBS solution that contained 30% sucrose and sodium azide (0.1%). Tissues were frozen in isopentane cooled in liquid nitrogen. The spinal cord and the dorsal ganglion specimens were mounted in medium.<sup>1</sup> Serial transverse sections of the spinal cord and longitudinal DRG sections (12- $\mu$ m thickness starting from the dorsal surface of the ganglion) were cut on a cryostat and mounted on gelatin-coated slides. A coverslip was not placed on the sections, and they were examined within 2 hours after cutting. Slides selected for immunohistochemistry were processed for immunostaining or stored at -20°C.

**Immunohistochemistry**—Immunohistochemical studies were performed only on frozen sections in which FB- or DY-stained neurons were previously observed. Preparations were preincubated in 10% normal goat serum in PBS solution that contained 1% Triton X-100 for 30 minutes at room temperature (approx 20°C) to decrease nonspecific binding and to make the tissue permeable. Primary antibodies against tis-

sue antigens were used (specifically, primary antibodies [rabbit, rabbit, mouse, and rabbit, respectively] against CGRP,<sup>8</sup> GAL,<sup>h</sup> NeuN,<sup>i</sup> and SP<sup>j</sup>), each at a dilution of 1:200. All primary antibodies were diluted in antibody diluent (1.8% NaCl in 0.01M sodium phosphate buffer that contained 0.1% sodium azide). Following incubation in single or combined primary antibodies for 1 night at 4°C in a humid chamber, preparations were given three 10-minute washes in PBS solution and then incubated for 1 hour at room temperature with appropriate secondary antibodies (specifically, goat anti-mouse<sup>k</sup> and goat anti-rabbit antibodies<sup>l</sup>) at a dilution of 1:200 and 1:40, respectively. Tissues were then washed further in PBS solution for three 10-minute periods and mounted in glycerol buffered with 0.5M sodium carbonate (pH, 8.6). The coverslips were sealed with clear nail varnish. To prove specificity of secondary antisera, they were applied without use of primary antibodies on bovine control spinal cord and ganglionic specimens. No staining was seen after omitting the primary antibodies.

**Fluorescence microscopy**—Sections were observed with a microscope<sup>m</sup> equipped with a filter system<sup>n</sup> that provides excitation light at a wavelength of 360 nm, which elicits the FB fluorescent labeling of the neuronal cytoplasm and DY labeling of the neuronal nucleus. The microscope was also equipped with the appropriate filter cubes for discriminating between the fluorescence of fluorescein isothiocyanate (FITC) and Alexa 594. For FITC, we used a 450- to 490-nm excitation filter and 515- to 565-nm emission filter<sup>o</sup>; for Alexa 594, we used a 530- to 585-nm excitation filter and 615-nm emission filter.<sup>p</sup> Images were recorded by use of a photo digital camera<sup>q</sup> and software program.<sup>r</sup> Contrast and sensitivity adjustment were performed by use of software programs.<sup>s,t</sup> Another software program<sup>u</sup> was used for the morphometric analysis of FB- or DY-labeled nerve cells sectioned through the nucleus. The somatic cross-sectional area of FB- and DY-labeled neurons was measured after manual tracing of the cell outline. Two hundred spinal cord and sensory FB- and DY-filled neurons (from 3 calves) were measured.

**Quantitative analysis**—The proportion of neurons that were positive for 1 of 2 retrograde tracers (FB and DY) and that were also immunoreactive for a particular neurochemical was determined by examining fluorescently labeled single-immunostained preparations. Neurons were first located by the presence of FB or DY staining, and then the filter was switched to determine whether the neuron was labeled for a particular antigen located with a fluorophore of a different color. Neurons with FB or DY labeling were counted, and their positivity or negativity for a particular marker was determined. One hundred efferent and afferent FB- and DY-positive neurons (from 3 calves) were counted for each neurochemical marker considered. The Student *t* test was used to evaluate differences between sizes of motoneurons that innervate the GM and FDSM and between sizes of DRG neurons that supply the same muscles. Values of *P* < 0.05 were considered as significant.

## Results

**Staining**—All FB- and DY-stained neurons were observed in the left ventral horns of the spinal cord and in the left DRG. The DY staining was observed also in the cytoplasm of some neurons; DY staining was often not only confined to the nucleus of the neurons but was also detectable in the small nuclei of the glial perineuronal cells. However, small nuclei of the glial perineuronal cells were distinguished from the nuclei of DY-stained neurons based on the fact that they were

oval in shape and were not surrounded by a fluorescently labeled cytoplasm. Furthermore, in spinal cord tissue, the DY-labeled motoneuron nuclei were far larger than labeled glial cells.

**Localization of FB-stained neurons**—Spinal cord FB-stained neurons were observed in Rexed's lamina IX of the L6, S1, and S2 segments. In particular, in 2 calves, FB-labeled neurons were present starting from the caudal half (lower part) of L6 up to the middle third of S2. Nevertheless, the main concentration of motoneurons that innervate the GM was always observed at the caudal half of the S1 segment and in the cranial third of the S2 segment. In 2 calves, the FB-stained neurons were observed only at the level of the S1 and S2 spinal cord segments. In 1 calf, the FB-stained neurons were observed also in the cranial part of the L6 segment but not in the S2 segment. The FB-stained cells were located dorsolaterally in the gray matter of the ventral horn in the L6 and S1 segments. In the middle third of the S2 spinal cord segment, the FB-stained cells were observed in the ventral horn. They were observed either in isolated positions or clustered in groups of 3 to 5 neurons. Their well-developed dendritic arborization remained inside the border of the motoneuronal column, and its main processes were oriented dorso-medially. In some sections, broad or narrow overlapping processes were visible but it was impossible to see any perikarya. The largest irregular or star-shaped somata had up to 5 broad processes emanating from them. The main processes were often divided into 2 or more narrower elongated daughter branches. The longest FB-stained processes could be followed for 200 to 300  $\mu$ m. The nuclei were generally located in the middle of the perikarya (Figure 1).

The FB-positive DRG cells were observed scattered within the DRG of L6-S2 segments. Calves that only had FB-positive GM motoneurons at the S1-S2 spinal cord levels had FB-stained sensory neurons at the same segments. It was possible to see no more than 8 to 12 FB-positive cells for each slice, and these were randomly distributed. The outline of these cells was sometimes irregular.

**Localization of DY-stained neurons**—Spinal cord DY-stained cells were observed at the L6-S2 levels. The DY-labeled neurons were present starting from the caudal third of L6 up to the cranial third of S2. The distribution pattern of the spinal cord DY-positive somata widely overlapped that of the FB-positive cells. At the L6 level, the DY-stained cells appeared a few micrometers cranially to the FB-stained neurons, and at the S2 level, they disappeared a few micrometers cranially to the lowest FB staining. It is worth noting that the number of DY-stained neurons detected was smaller than the number of FB-stained cells and that the DY-stained neurons generally occupied a lateral or dorsolateral position in respect to FB-stained perikarya (Figures 1 and 2). Morphometric evaluation was also possible in the DY-positive cells because of the frequent cytoplasmic DY staining and the DY staining of pericellular glial cell nuclei, which permitted the exact definition of pericellular neuronal borders. Perineuronal glial



labeling was probably the result of postmortem translocation of dye during aqueous procedures of the immunohistochemical processing,<sup>28</sup> although an *in vivo* migration of the dye cannot be excluded.

The DY-positive cells were present along the DRGs of L6-S2. In each ganglion section, it was possible to detect only a few scattered DY-stained neurons.

**Soma size of retrogradely labeled neurons**—Motoneurons stained with the 2 fluorescent tracers had a wide range of dimensions. The FB-positive neurons were between 759 and 4,642  $\mu\text{m}^2$  in cross-sectional area, and the largest FB-positive neurons were generally more numerous than the largest DY-labeled neurons (range, cross-sectional area of 735 to 4,193  $\mu\text{m}^2$ ). Mean ( $\pm$  SD) value of the cross-sectional area of the spinal cord FB- and DY-stained somata was 2,838  $\pm$  777  $\mu\text{m}^2$  and 2,460  $\pm$  705  $\mu\text{m}^2$ , respectively (Figure 3). Mean soma size of motoneurons that innervate the GM significantly ( $P < 0.001$ ) differed from those that supply the FDSM (Figure 4). The FB-filled neurons with a major axis  $> 100 \mu\text{m}$  in length were 10% of the total neuronal population considered (compared with only 1.5% of DY-labeled cells). Furthermore, we observed a few gamma-motoneurons that supply GM and FDSM (1.5% and 3.5%, respectively); we considered these cells as gamma motoneurons because of their small dimension.

The muscle afferent population of sensory neurons had obvious small (cross-sectional area of 791 and 797  $\mu\text{m}^2$  for FB- and DY-positive neurons, respectively), medium, and large (cross-sectional area of 5,876 and 6,653  $\mu\text{m}^2$  for FB- and DY-positive neurons, respectively) peaks in the distribution of the cell sizes, with the medium and small cell peaks being more dramatic. Mean value of the cross-sectional area of FB- and DY-stained DRG somata was 2,367  $\pm$  1,012  $\mu\text{m}^2$  and 2,328  $\pm$  1,123  $\mu\text{m}^2$ , respectively (Figure 3). The difference between the mean soma size of DRG neurons that supply the GM and FDSM was not significant ( $P = 0.71$ ; Figure 4). The FB- and DY-stained neurons had a major axis in the range of 38 to 109  $\mu\text{m}$  and 37 to 118  $\mu\text{m}$  in length, respectively.

**Accessory ganglion**—In 1 calf, the presence of a small sympathetic ganglion associated with the DRG at the S1 level was observed. The numerous FB- (28 to 34 cells/section) and less numerous DY-stained neurons were smaller in size in comparison to the DRG neurons. These neurons, which were closely located to the DRG neurons (but not intermingled), were not immunoreactive for the neurochemical markers used in this investigation. The FB staining indicated that these neurons were not pseudounipolar in shape; they were similar in appearance to multipolar neurons (Figure 5). Their cross-sectional area (approx 700  $\mu\text{m}^2$ ) corresponded, in fact, to that of neurons observed typically in the sympathetic paravertebral ganglia in cats.<sup>29</sup> We also performed a collateral immunostaining investigation by use of a rabbit antiserum<sup>v</sup> (dilution of 1:40) raised against dopamine- $\beta$ -hydroxylase and observed a high degree of dopamine- $\beta$ -hydroxylase immunoreactivity in the neuronal population of that ganglion but not that of the DRG neurons. A similar accessory ganglion

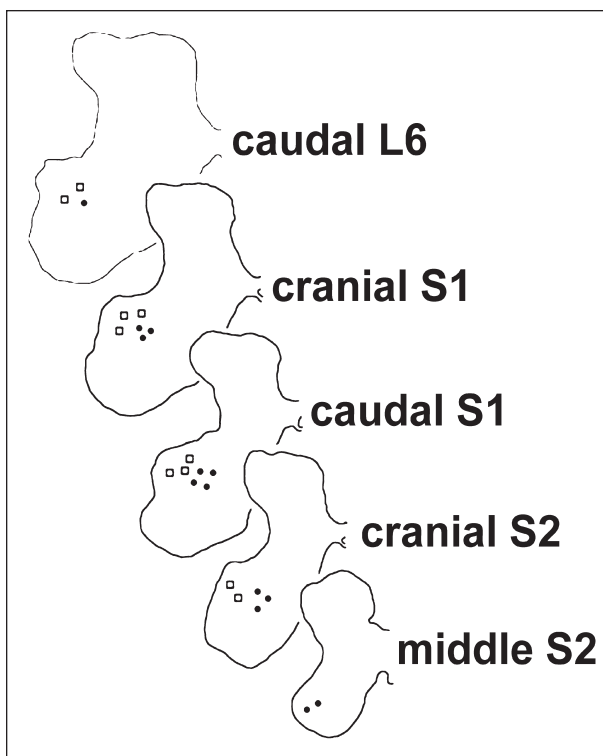


Figure 1—Schematic diagram of cross sections at representative levels throughout the craniocaudal extent of the L6-S2 spinal cord segment that illustrate the distribution in the ventral horn of labeled neurons following injections of fluorescent tracers (fast blue [FB] and diamidino yellow dihydrochloride [DY]) in the gastrocnemius muscle (GM) and superficial digital flexor muscle (FDSM). The FB- (closed circles) labeled motoneurons innervate the GM; the DY- (open squares) labeled motoneurons innervate the FDSM. Number of circles and squares does not reflect the exact number of the labeled cells but indicates the relative densities at different levels of the spinal cord. Notice that the FDSM motoneurons occupy a lateral or dorsolateral position in respect to GM motoneurons.

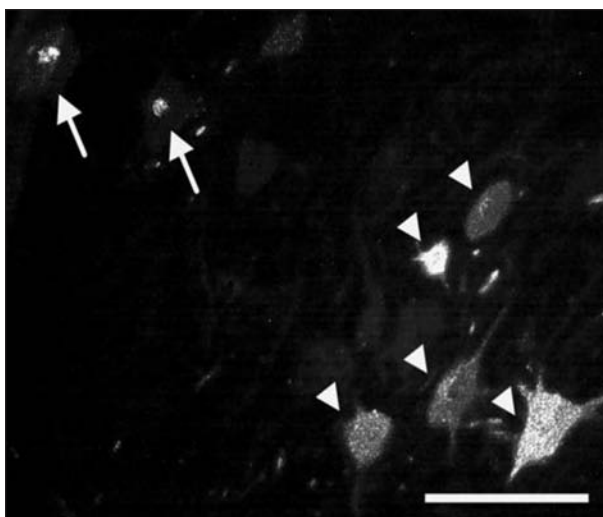


Figure 2—Photomicrograph of a section of neurons retrogradely labeled with FB (arrowheads) and DY (arrows) in Rexed's lamina IX in the left ventral horn of the S1 segment of the spinal cord following injections of FB (2%) and DY (2%) into the GM and FDSM, respectively. The DY-labeled neurons occupy a dorsolateral position in respect to FB-stained perikarya. Bar = 200  $\mu\text{m}$ .

has already been observed at the lumbar level associated with ventral roots<sup>w</sup> but never at the sacral level and not in cattle. It is interesting to note that Ramer and Bisby,<sup>30</sup> studying neuropathic pain derived by sympathetic-sensory interaction, found pericellular baskets composed of tyrosine hydroxylase immunoreactive fibers all around a subpopulation of DRG neurons. The presence of this closely located sympathetic ganglia leads us to suggest that a putative source of this innervation could be the neurons of sympathetic trunk ganglia or DRG-associated accessory ganglia. The presence of sympathetic ganglion cells in close proximity to DRG cells could be the result of a lack of differential migration of the neural crest cells which ultimately give origin to both the sympathetic postganglionic neurons and the primary afferent neurons. The accessory ganglia could also be small sympathetic trunk ganglia that, because of the ascent of the cord during the development, have followed the lumbosacral DRG into the vertebral canal.

**Neurochemical code of spinal motor neurons**—No FB- or DY-stained neurons were immunoreactive for TK. Along the borders of many somata and main processes of FB- and DY-labeled neurons, some small TK immunoreactive varicosities were visible, and these probably belonged to TK immunoreactive afferents. A substantial percentage of FB- (79%) and DY- (73%) positive motoneurons detected in the lamina IX of spinal segments L6-S2 was CGRP positive. The CGRP cytoplasmic staining was homogeneously distributed in a granular pattern within the cell bodies and sometimes extended out into broad proximal dendrites (Figure 5). No FB- or DY-stained neurons had GAL immunoreactivity.

**Neurochemical code of sensory neurons**—Ganglionic FB- and DY-positive neurons with TK immunoreactivity were numerous (35% and 29%, respectively). The TK staining was almost always strongly expressed in small cells (Figure 5). The FB- and DY-positive cells expressed the same degree (ie, 60%) of CGRP immunoreactivity. The CGRP immunoreactivity was present in cells as a diffuse labeling throughout the cytoplasm. It was observed in cells of all sizes but was more strongly detected in small neurons. It was also possible to see some CGRP immunoreactivity fibers that ran between positive or negative somata. About 50% of the FB- and DY-stained somata had faint GAL immunoreactivity (51% and 48%, respectively). Only a few small DY cells had strong GAL immunoreactivity. The strongest GAL

immunoreactivity was found mainly for a few small neurons scattered throughout the ganglia. Typical GAL-positive pericellular basket-like structures around GAL-positive and GAL-negative perikarya were observed. Immunoreactivity to NeuN was present in the cytoplasm and nucleus of many DRG neurons, but it was not observed in FB- and DY-stained somata. In fact, 61% of the FB-stained neurons also had NeuN immunoreactivity, whereas only 31% of DY-stained cells were NeuN immunoreactive.

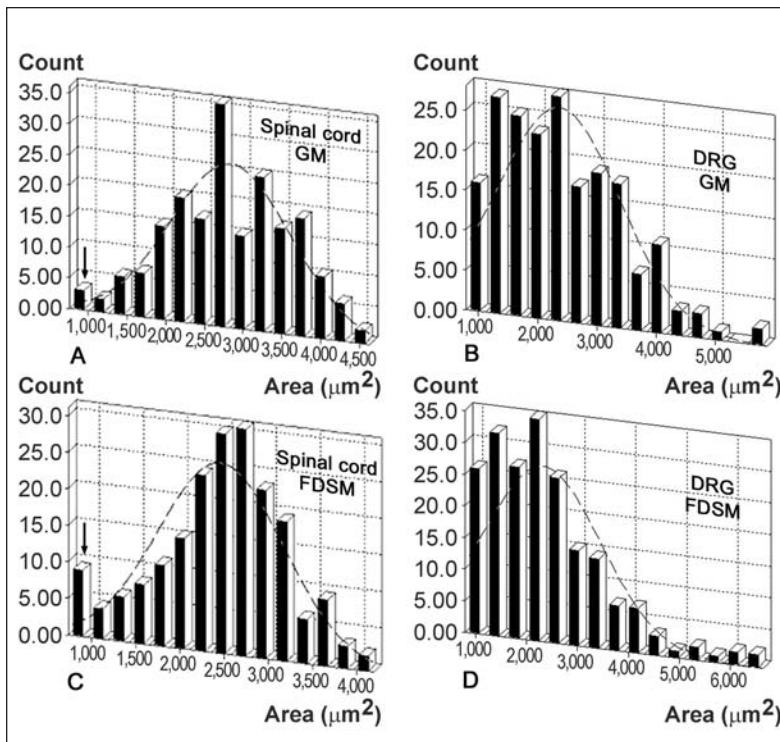


Figure 3—Frequency distributions of cross-sectional soma areas of 200 motoneurons (panels A and C) and 200 ganglion cells (panels B and D) that supply the GM and FDSM in cattle. Mean ( $\pm$  SD) cross-sectional area of GM and FDSM motoneurons was  $2,838 \pm 777 \mu\text{m}^2$  and  $2,460 \pm 705 \mu\text{m}^2$ , respectively, whereas the mean value of the cross-sectional area of dorsal root ganglion (DRG) neurons of the GM and FDSM was  $2,367 \pm 1,012 \mu\text{m}^2$  and  $2,328 \pm 1,123 \mu\text{m}^2$ , respectively. Motoneurons that supply the GM and FDSM with soma areas of  $< 900 \mu\text{m}^2$  (arrows) were 1.5% and 3.5%, respectively; these populations of cells are presumed to represent the gamma-motoneuron population.

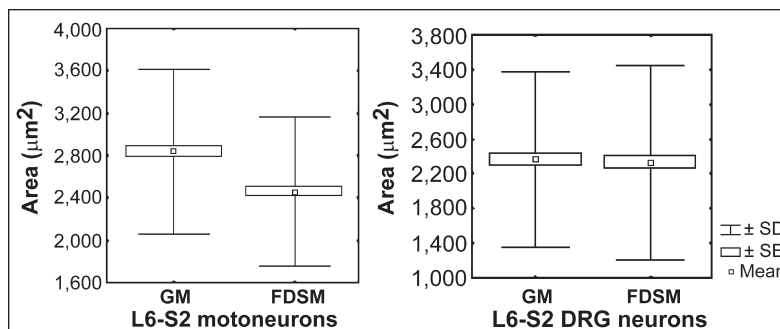


Figure 4—Box-and-whisker plots of soma areas of motoneurons (left) that supply the GM and FDSM and of sensory neurons (right) of the DRG that supply the GM and FDSM. Mean cross-sectional area of motoneurons that innervate the GM ( $2,837.62 \mu\text{m}^2$ ) is significantly ( $P < 0.001$ ) greater than the mean soma size of those that supply the FDSM ( $2,459.86 \mu\text{m}^2$ ). Mean soma size of DRG neurons that innervate the GM ( $2,366.82 \mu\text{m}^2$ ) did not differ from the mean soma area of those that supply the FDSM ( $2,328.38 \mu\text{m}^2$ ).

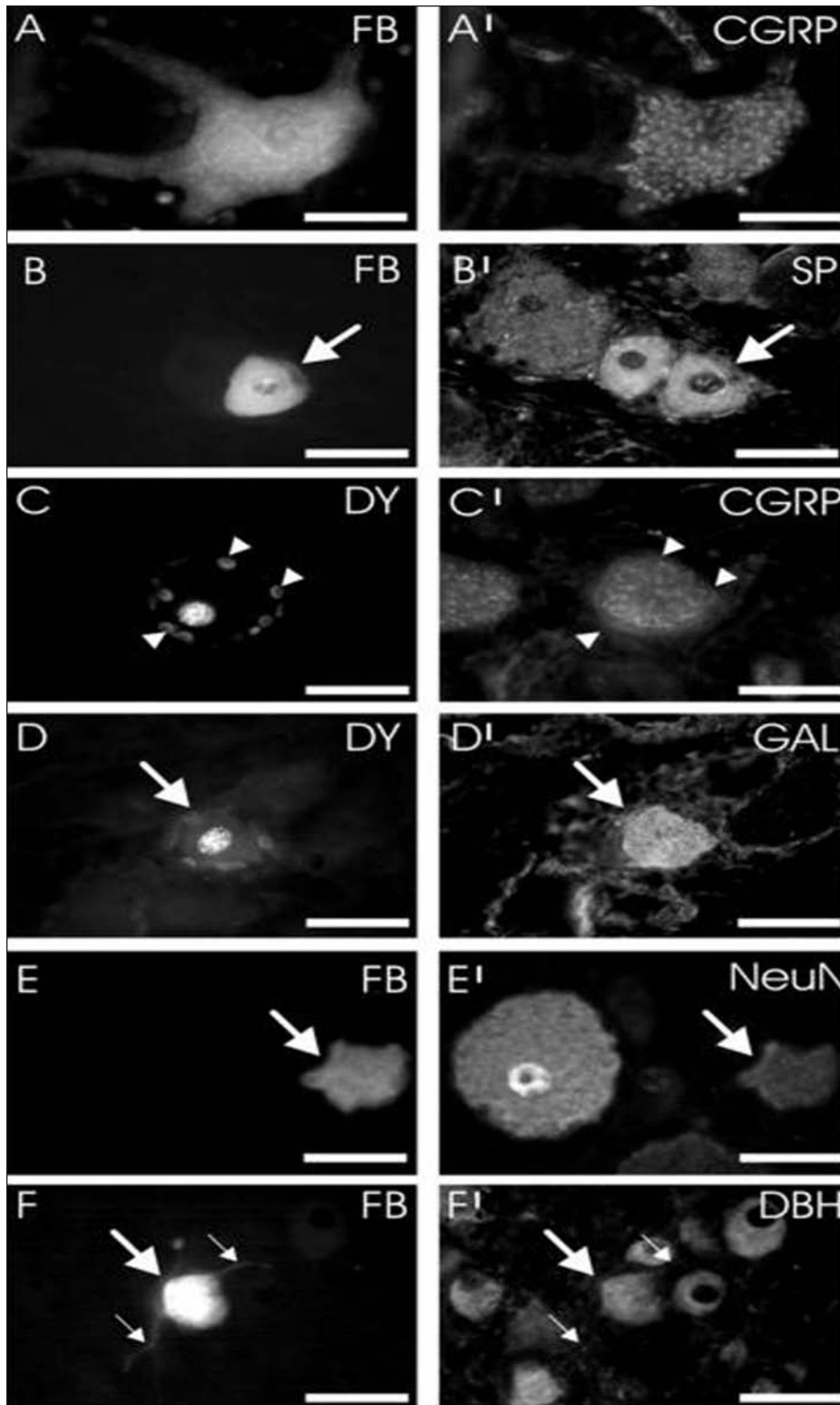


Figure 5—Photomicrographs of calcitonin gene-related peptide (CGRP)-, substance P (SP)-, galanin (GAL)-, neuronal nuclear protein (NeuN)-, and dopamine- $\beta$ -hydroxylase (DBH)-immunoreactivity in neurons labeled after injection of FB (2%) and DY (2%) into the GM and FDSM, respectively. A–A'—An FB-labeled motoneuron (A) from the left S2 segment of the spinal cord with strong cytoplasmic CGRP staining (A') distributed in a granular pattern within the cell bodies that also extended into the broad proximal dendrites. B–B'—A small FB-labeled DRG neuron (B; arrows) of the S1 segment that was strongly SP immunoreactive (B'). C–C'—Nuclei that are DY-labeled and belong to the glial cells that encircle (arrowheads) a DY-labeled DRG neuron (C) of the S1 segment that was immunoreactive for CGRP (C'). D–D'—A DY-labeled DRG neuron (D; arrows) of the S1 segment that was immunoreactive for GAL (D'). Notice that the DY staining could also be observed in the cytoplasm of some neurons and that only the small cells had strong GAL immunoreactivity. E–E'—An FB-labeled DRG neuron (E; arrows) that was also NeuN immunoreactive (E'). F–F'—An FB-labeled multipolar DRG neuron (F; large arrows) observed at the level of the S1 segment but belonging to an accessory sympathetic ganglion associated with the DRG; notice the presence of 2 neuronal processes (small arrows). The DRG-associated accessory ganglion was composed of neurons that were immunoreactive for DBH(F'). Bars = 50  $\mu$ m.

## Discussion

The 2 fluorescent tracers used in our study have already been used (crystals applied to sciatic nerve) to study the peripheral nervous system, and it has been shown that there are no quantitative differences between the number of motor and sensory neurons that are stained by use of application of the 2 dyes in

the same neuronal pathway.<sup>11</sup> The methods used in our study do not allow an unbiased estimate of the true number of neurons of each muscle, but despite the large dimension of muscles and the relative small amount of tracers used, we believe that the exact distribution of the neurons has been observed.

It is worth noting that our investigation on the



localization of afferent and efferent neurons that supply the GM and FDSM was not performed by application of dye after axotomy of the nerves reaching these muscles. We believe that the procedure that we have used did not alter either the cellular sizes or their immunoreactivity. Also, if the dye was in the cells for longer before fixation, it did not noticeably affect these parameters.

The results obtained from our study regarding the position of the GM efferent neurons are partially in agreement with an earlier description of neurons in the lumbosacral region of the spinal cord.<sup>31</sup> Goller<sup>31</sup> concluded that the L6-S2 segments were the origin of the sciatic nerve fibers in cattle, but no data were available about the origin of the tibial nerve, which is one of its branches. Results of a recent study<sup>11</sup> performed in rats by use of the fluorescent tracers FB and DY revealed that the spinal cord and DRG neurons that project their fibers to the sciatic nerve are located at the L4-L6 levels. It has been proposed that in spastic paresis, an excessive activity of the muscle spindle reflex arc mechanism is involved. The selective resection of the GM afferent nerves, which contain the Ia afferents from muscle spindles, relieved the clinical signs in 3 calves.<sup>15</sup> Involvement of other muscular groups in spastic paresis needs to be considered. In our study, we also studied another hind limb muscle, the FDSM, but we can assume on the basis of the clinical signs that many other muscles are involved in the spastic paresis of calves, especially in chronic situations. The involvement of the GM and FDSM clearly appears at the beginning of the disease. In more progressive phases of the disorder, 1 or both of the hind limbs appear to be fully extended and many other muscular groups must be involved to achieve this. In addition to these signs, the forelimb and neck muscles may be contracted in the advanced stages of the disease. The FB- and DY-stained neurons were present at the L6 (in 3 calves), S1, and S2 spinal cord levels. Our results indicate that extensive overlap exists in the spatial distribution of motoneurons that innervate the 2 muscles considered. When both FB- and DY-stained neurons are observed at the L6 level, DY-positive neurons appeared cranially to FB fluorescent cells and disappeared cranially to the FB-positive neurons at the S2 level. A cranial-to-caudal topographic distribution for each muscle existed, indicating that the motor nuclei of the 2 muscles are organized by a somatotopic pattern. To our knowledge, our study is the first in cattle to determine the location and extent of the neurons that supply the GM and FDSM. In the past, Wells et al<sup>20</sup> showed that the cattle tibial nerve had the source of its fibers only in the L6 spinal cord segment. Vanderhorst and Holstege<sup>10</sup> localized motoneurons that innervate the GM and the flexor digitorum longus muscle at the L7-S1 spinal cord level in cats. Thomas et al<sup>32</sup> investigated the spinal cord localization of neurons that innervate a small muscle of the rat hind limb, the flexor digitorum superficialis brevis digiti quinti, with an FB fluorescent tracer and observed that the FB-stained neurons were located laterally in the ventral horn of the L4-L6 levels. Byers et al<sup>11</sup> recognized the source of fibers that reach the GM at the L4-L6 spinal cord levels in rats. In our study, cattle

GM motoneurons were located in a rather compact cell group in the dorsolateral part of the ventral horn. Motoneurons that innervate the FDSM were located dorsolaterally to the GM motoneurons.

Despite what has been reported on the DRG of rats,<sup>32-34</sup> we did not observe any somatotopic organization of primary afferent neurons. However, there are several indications that there may be a DRG somatotopic organization.<sup>33-35</sup> Peyronnard et al<sup>36,37</sup> reported that afferent neurons from different rat hind limb muscles tend to form a separate cluster in lumbar DRG.

We observed that the neurons stained with the 2 fluorescent tracers had a similar range of dimensions but that the largest FB-positive neurons were generally more numerous than the largest DY-positive neurons. To understand these differences between motoneuron sizes, we need to consider the function of the 2 muscles investigated: the GM is less involved than FDSM in antigravity function. In consideration of the motoneuron size principle, Henneman et al<sup>38</sup> suggested that the size of a cell determines its threshold and that the largest cells of a motoneuronal pool are seldom fired in the course of postural activities.

Because no data are available on the dimension of cattle gamma neurons, we must compare our data with that obtained in other species. Mean diameter of gamma cell bodies in the lumbosacral region of the spinal cord that send their fibers into the sciatic nerve was calculated to be between 25.5 and 37.5  $\mu\text{m}$  in cats.<sup>39</sup> Rat ventral horn neurons of the L5 segment with a cell body size smaller than 491  $\mu\text{m}^2$  (ie, 25  $\mu\text{m}$  in diameter) were presumed to be gamma motoneurons that innervate intrafusal muscle fibers within the muscle spindle.<sup>40</sup> On the basis of these observations and on analysis of the somatic cross-sectional area of the neurons retrogradely labeled from the GM and FDSM in our study, we can state that we recognized perikarya, which could be considered to belong to the gamma neuron subclass on the basis of their dimension. Nevertheless, we observed more putative DY gamma-positive neurons; these data can be justified by the fact that FDSM is more involved in postural function than GM.

A number of morphologic studies have been devoted to the postnatal development of mammalian alpha motoneurons. The results from studies on the postnatal growth of the cell body seem to indicate that the cell body volume of the triceps surae alpha motoneurons of newborn kitten should be approximately a third<sup>3</sup> or a fourth<sup>1</sup> of the volume in adult cats. In the Cullheim and Ulfhake<sup>3</sup> investigation, kitten motoneurons reached the adult value at 44 to 46 days of postnatal age. There are no similar studies on cattle spinal cord motoneurons, but comparatively, we can suppose that at the age in which calves of our investigation have been euthanatized (3 to 6 months of age), neurons were fully developed. Also, the mean volume of the DRG nerve cell bodies is greater in older mammals than in young adults, and this is probably related to the larger body size of the old animals.<sup>41</sup>

Tachykinin has been found in somatic (nociceptive) afferent neurons<sup>42</sup> and in visceral neuronal pathways.<sup>43</sup> About 50% of DRG neurons labeled with FB

and DY had TK immunoreactivity; our results are in agreement with those obtained in rats by Perry and Lawson,<sup>26</sup> who observed that 51% of the FB-positive DRG neurons were SP immunoreactive after FB application on the cut GM nerve. In skeletal muscle, both SP and CGRP have effects of vasodilation on arterioles. The sustained proportions of muscle afferent TK immunoreactive neurons suggest a role for TK peptide in the regulation of microcirculation in muscle also in cattle. It is possible that TK could be limited to the nociceptive group III and group IV muscle afferent neurons because TK was absent in muscle spindle afferent neurons in guinea pig.<sup>42</sup>

As a 37-amino acid peptide that results from the alternative splicing of mRNA transcribed from the calcitonin gene, CGRP has a wide distribution in the CNS that includes the sensory and motor system of the spinal cord. Motoneuron somata in cranial as well as spinal motor pools are CGRP positive in a variety of species, including frogs, chicks, rats, guinea pigs, monkeys, and humans.<sup>44-49</sup> The supposed physiologic functions of CGRP in the regulation of motor function is at the developing or regenerating neuromuscular junction. During development, CGRP promotes myotube differentiation and the upregulation of nicotinic acetylcholine receptors. In the normal adult skeletal muscle, CGRP also enhances the force of twitch muscle contraction by approximately 30% to 50%.<sup>x</sup> The distribution of CGRP in the motoneurons that innervate the hind limb muscles has been analyzed in rats<sup>50-52</sup> and in cats.<sup>53</sup> Findings in the study of Piehl et al<sup>50</sup> revealed that not all of the motoneuron pools inside the spinal cord have the same CGRP immunoreactivity, or rather there are also some CGRP-negative neurons, which belonged to the slow motor units. Results of a recent investigation<sup>y</sup> on myofibrillar adenosine triphosphatase and nicotinamide adenine dinucleotide tetrazolium reductase histochemistry revealed that 86% of the fibers of GM from healthy cattle were fast twitch fibers (ie, highly fatigable fibers [type II fibers]). This could explain the mean values of 80% (FB) and 73% (DY) of stained neurons with CGRP immunoreactivity following GM injection. Future investigation of CGRP immunoreactivity in spinal cord motoneurons of calves affected with spastic paresis will be of interest, as we already know that in affected cows, there is a dramatic reduction in the type II muscle fiber composition in the GM. In affected calves, type II muscle fibers make up only 26% of the total muscle fiber number, compared with 86% in control calves.<sup>y</sup> At the same time, there is a significant increase in the percentage of type I fibers, increasing from 13% to 25% in control calves to 51% to 57% in affected calves. These results are similar to that already observed in the GM of humans with spastic paresis,<sup>54</sup> where the authors detected histochemical changes in fiber type, with atrophy of type II fibers and hypertrophy of type I fibers. In summary, during spastic paresis, there is a clear transformation of the highly fatigable fibers (type II) into slow twitch, fatigue-resistant fibers. The reduction of CGRP immunoreactivity in motoneurons has been shown after removing the supraspinal descending projections to motoneurons.<sup>55</sup> We agree with Sheean,<sup>56</sup> who main-

tains that one of the most important reasons for the development of spastic paresis could be an altered equilibrium between the descending extrapyramidal (vestibulospinal, rubrospinal, and reticulospinal) pathways that regulate the extensor and flexor muscle activity by acting on alpha and gamma motoneurons. Sheean<sup>56</sup> suggests that human spasticity is only one of several components of the upper motor neurone syndrome; upper motor neurones include supraspinal inhibitory and excitatory fibers, which descend to the spinal cord, thereby exerting a balanced control on spinal reflex activity. Despite the success of deafferentation,<sup>15</sup> some doubts remain as to whether a descending pathway control could alter existing disease. This is suggested by the fact that all joints of the affected limb could be manually flexed without causing pain, but they returned to full extension as soon as the manipulation ceased.<sup>57</sup> This could indicate that the extensor muscle motoneurons are normally activated and that the flexor motoneuron pool is underactivated.

Release of CGRP from primary afferent neurons may increase excitability in some neurons of the spinal dorsal horn, perhaps by potentiating the release of SP or the effects of released SP,<sup>58</sup> thereby contributing to sensitization of the central nociceptive pathway. Release of CGRP peptide from peripheral terminals of primary afferent neurons contributes to local inflammatory responses that cause local vasodilatation and an increase in plasma extravasation produced by SP.<sup>59-61</sup> In rats, CGRP immunoreactivity in the DRG is present in all sizes of neuronal somata, including those with C, A $\delta$ , and A $\alpha$ / $\beta$  fibers.<sup>62</sup> Results of a study by Lawson et al<sup>63</sup> that coupled electrophysiology and immunohistochemistry in the DRG of guinea pigs revealed that no muscle spindle sensory neurons at the L5-S1 ganglionic levels were CGRP immunoreactive, whereas CGRP immunoreactivity was evident in ganglionic somata that supply skeletal muscle. The CGRP expression was detected in less than half of nociceptive neurons but was not limited to this neuron type. A small number of high and low threshold mechanoreceptive neurons with CGRP immunoreactivity have been described in rat DRG neurons.<sup>64</sup> Somata that are CGRP immunoreactive possessed receptive endings in the skin and deep somatic tissues, such as muscles, fasciae, tendons, and joints. In our study, we observed that about 60% of retrogradely traced neurons were CGRP immunoreactive and that the small somata had the strongest CGRP immunoreactivity; nevertheless, we are not able to distinguish between muscle spindle sensory and skeletal sensory muscle neurons.

The 29-amino acid peptide GAL is widely distributed in the mammalian nervous system. Although the function of GAL in motoneurons is currently unknown, the presence of GAL immunoreactivity has been observed in spinal cord motoneurons of rats.<sup>45,65</sup> In contrast to normal adult motoneurons, which express little or no GAL mRNA,<sup>66</sup> high levels of peptide immunoreactivity and messages are observed during development and following motoneuron injury; this may be because GAL plays a role in motoneuron regeneration. This probably reflects a peculiar role for this



peptide. In our investigation, as with observations in the horse and the pig,<sup>25</sup> no GAL immunoreactivity was found in healthy L6-S2 spinal cord motoneurons.

The GAL-like immunoreactivity and GAL receptors were found in DRG cells and in dorsal horn interneurons, suggesting that this neuropeptide may have a role in sensory transmission and modulation at the spinal level. Under normal conditions, GAL occurs in a small population of primary sensory neurons as well as in spinal interneurons. However, following peripheral nerve injury or inflammation, expression of GAL in primary afferents and spinal cord is upregulated.<sup>67</sup> It has been observed that following partial sciatic nerve injury, there was an upregulation in medium and large DRG cells.<sup>68</sup> We observed that about half of FB- or DY-stained cells were GAL immunoreactive, and we also observed immunoreactivity in pericellular baskets. We do not know whether there were only perineuronal reactive glial cells or also reactive fibers around these neurons.

Anti-NeuN serum has been reported to be a general neuronal nuclear marker, which stains almost all of the vertebrate neuronal types.<sup>69</sup> It has been demonstrated that NeuN antiserum may also stain the cytoplasm of intrinsic primary afferent neurons in the enteric nervous system of the guinea pig intestine,<sup>70,z</sup> and this antibody can therefore be used as a selective marker for intrinsic primary afferent neurons. With this antibody, we observed that in bovine DRG neurons, the NeuN antibody labeled both the cytoplasm and nucleus of many cells. We found that almost all NeuN immunoreactive neurons were also GAL immunoreactive.

In conclusion, the evaluation of the topography, morphology, and neurochemical code of neurons that innervate the GM and FDSM could be useful in a comparative analysis between healthy and diseased calves.

- a. Hamoir J. La contracture des Muscles Jumeaux chez le bœuf (abstr). *Echo Vét* 1922;51:63.
- b. Götz R. Spastische Parese der hinteren Extremität bei Kälbern und Junggrindern (abstr). *Deutsche Tierärztliche Wochenschrift* 1932;40:197:200.
- c. Grandis A, Bombardi C, Clavenzani P, et al. Innervazione dei muscoli estensori del piede nel bovino. Localizzazione e studio immunostochimico della componente motoria e sensitiva (abstr). *Atti LVII Conv. Naz. S.I.S.Vet., Ischia* 2003;19.
- d. Sigma-Aldrich Chemie, Steinheim, Germany.
- e. Sigma-Aldrich Chemie, Steinheim, Germany.
- f. Tissue Tek, Sakura Finetek Europe, Zoeterwoude, The Netherlands.
- g. Peninsula Laboratories Inc, San Carlos, Calif.
- h. Peninsula Laboratories Inc, San Carlos, Calif.
- i. Chemicon International, Temecula, Calif.
- j. Diasorin Industrial Boulevard, Stillwater, Minn.
- k. Molecular Probes, Eugene, Ore.
- l. Calbiochem, Novabiochem Corp, San Diego, Calif.
- m. Axioplan epifluorescence microscope, Carl Zeiss, Oberkochen, Germany.
- n. Filter system A, Carl Zeiss, Oberkochen, Germany.
- o. Filter set 10, Carl Zeiss, Oberkochen, Germany.
- p. Filter set 00, Carl Zeiss, Oberkochen, Germany.
- q. DMC, Polaroid Corp, Cambridge, Mass.
- r. DMC2, Polaroid Corp, Cambridge, Mass.
- s. Corel photo paint, Ottawa, ON, Canada.
- t. Corel draw, Ottawa, ON, Canada.
- u. KS300 Zeiss, Kontron Elektronik, Munich, Germany.
- v. Biogenesis Ltd, Poole, Dorset, UK.
- w. Alexander WP, Kuntz A, Henderson WP, et al. Sympathetic ganglion cells in ventral roots. Their relation to sympathectomy (abstr). *Science* 1949;109:484.
- x. Ohhashi T, Jacobowitz DM. Effects of calcitonin gene-related peptide on neuromuscular transmission in the isolated rat diaphragm (abstr). *Peptides* 1988;9:613.
- y. Barazzoni AM, Bompadre G, Grandis A, et al. Histochemical aspects of gastrocnemius muscle fibers in healthy and spastic paresis affected bovine (abstr), in *Proceedings. 4th Cong Naz Assoc Ital Morfol Vet* 2003;21.
- z. Brody KM, Costa M, Brookes SJH. Neu-N immunoreactivity marks primary afferent neurons in the guinea-pig submucous plexus (abstr). *Proc Aust Neurosci Soc* 2002;13:105.

## References

1. Sato M, Mizuno N, Konishi A. Postnatal differentiation of cell body volumes of spinal motoneurons innervating slow-twitch and fast-twitch muscles. *J Comp Neurol* 1977;175:27–36.
2. Burke RE, Strick PL, Kanda K, et al. Anatomy of medial gastrocnemius and soleus motor nuclei in cat spinal cord. *J Neurophysiol* 1977;40:667–680.
3. Cullheim S, Ulfhake B. Relations between cell body size, axon diameter and axon conduction velocity of triceps surae alpha motoneurons during the postnatal development in the cat. *J Comp Neurol* 1979;188:679–686.
4. Kellerth JO, Berthold C-H, Conradi S. Electron microscopic studies of serially sectioned cat spinal  $\alpha$ -motoneurons. III. Motoneurons innervating fast-twitch (type FR) units of the gastrocnemius muscle. *J Comp Neurol* 1979;184:755–767.
5. Weeks OI, English AW. Compartmentalization of the cat lateral gastrocnemius motor nucleus. *J Comp Neurol* 1985;235:255–267.
6. Weeks OI, English AW. Cat triceps surae motor nuclei are organized topologically. *Exp Neurol* 1987;96:163–177.
7. Molander C, Ygge J, Dalsgaard CJ. Substance P-, somatostatin- and calcitonin gene-related peptide-like immunoreactivity and fluoride resistant acid phosphatase-activity in relation to retrogradely labeled cutaneous, muscular and visceral primary sensory neurons in the rat. *Neurosci Lett* 1987;74:37–42.
8. Swett JE, Torigoe Y, Elie VR, et al. Sensory neurons of the rat sciatic nerve. *Exp Neurol* 1991;114:82–103.
9. Swett JE, Wikholm RP, Blanks RH, et al. Motoneurons of the rat sciatic nerve. *Exp Neurol* 1986;93:227–252.
10. Vanderhorst VG, Holstege G. Organization of lumbosacral motoneuronal cell groups innervating hindlimb, pelvic floor, and axial muscles in the cat. *J Comp Neurol* 1997;382:46–76.
11. Byers CT, Fan R, Messina A, et al. Comparing the efficacy of two fluorescent retrograde tracers in labeling the motor and sensory neuron populations of the rat sciatic nerve. *J Neurosci Methods* 2002;114:159–164.
12. Roberts SJ. Hereditary spastic diseases affecting cattle in New York State. *Cornell Vet* 1965;55:637–644.
13. Ledoux M. Bovine spastic paresis: etiological hypotheses. *Med Hypotheses* 2001;57:573–579.
14. Ledoux JM. Hypothesis of interference to superinfection between bovine spastic paresis and bovine spongiform encephalopathy; suggestions for experimentation, theoretical and practical interest. *Med Hypotheses* 2004;62:346–353.
15. De Ley G, De Moor A. Bovine spastic paralysis: results of surgical desafferentation of the gastrocnemius muscle by means of spinal dorsal root resection. *Am J Vet Res* 1977;38:1899–1900.
16. Mayhew IG, ed. *Large animal neurology: a handbook for veterinary clinicians*. Philadelphia: Lea & Febiger, 1989;216.
17. Vlaminck L, De Moor A, Martens A, et al. Partial tibial neurectomy in 113 Belgian blue calves with spastic paresis. *Vet Rec* 2000;147:16–19.
18. Pavaux CL, Sautet J, Lignereux Y. Anatomie du muscle gastrocnémien des bovins appliquée a la cure chirurgicale de la parésie spastique. *Vlaams Diergeneeskd Tijdschr* 1985;54:296–312.
19. De Ley G, De Moor A. Bovine spastic paralysis: results of selective  $\gamma$ -efferent suppression with dilute procaine. *Vet Sci Comm* 1980;3:289–298.

20. Wells GA, Hawkins SA, O'Toole DT, et al. Spastic syndrome in a Holstein bull: a histologic study. *Vet Pathol* 1987;24:345-353.
21. Troyer D, Leipold HW, Cash W, et al. Upper motor neurone and descending tract pathology in bovine spinal muscular atrophy. *J Comp Pathol* 1992;107:305-317.
22. Pumarola M, Añor S, Majó N, et al. Spinal muscular atrophy in Holstein-Friesian calves. *Acta Neuropathol (Berl)* 1997;93:178-183.
23. Pietrowski D, Goldammer T, Meinert S, et al. Description and physical localization of the bovine survival of motor neuron gene (SMN). *Cytogenet Cell Genet* 1998;83:39-42.
24. Sisó S, Pumarola M, Ferrer I. Cell death and decreased synaptic protein expression in the ventral horn of Holstein-Friesian calves with spinal muscular atrophy. *J Comp Pathol* 2003;128:132-139.
25. Merighi A, Kar S, Gibson SJ, et al. The immunocytochemical distribution of seven peptides in the spinal cord and dorsal root ganglia of horse and pig. *Anat Embryol (Berl)* 1990;181:271-280.
26. Perry MJ, Lawson SN. Differences in expression of oligosaccharides, neuropeptides, carbonic anhydrase and neurofilament in rat primary afferent neurons retrogradely labelled via skin, muscle or visceral nerves. *Neuroscience* 1998;85:293-310.
27. Chiocchetti R, Clavanzani P, Barazzoni AM, et al. Viscerotopic representation of the subdiaphragmatic tracts of the digestive apparatus within the vagus complex in the sheep. *Brain Res* 2003;961:32-44.
28. Bentivoglio M, Kuypers HG, Catsman-Berreoets CE. Retrograde neuronal labeling by means of bisbenzimidazole and nuclear yellow (hoechst 5769121). Measures to prevent diffusion of the tracers out of retrogradely labeled neurons. *Neurosci Lett* 1980;18:19-24.
29. Percy WH, Walsh J, Krier J. Morphological and electrophysiological properties of cat lumbar paravertebral neurones. *J Auton Nerv Syst* 1988;24:183-192.
30. Ramer MS, Bisby MA. Sympathetic axons surround neuropeptide-negative axotomized sensory neurons. *Neuroreport* 1998;9:3109-3113.
31. Goller H. Kerngebiete des rinderrückenmarkes. *Zentralbl Veterinarmed [A]* 1962;1:52-66.
32. Thomas CK, Esipenko V, Xu XM, et al. Innervation and properties of the rat FDSBQ muscle: an animal model to evaluate voluntary muscle strength after incomplete spinal cord injury. *Exp Neurol* 1999;158:279-289.
33. Wessels WJ, Feirabend HK, Marani E. Somatotopic organization in the sensory innervation of the rat hindlimb during development, using half dorsal root ganglia as subsegmental units. *Eur J Morphol* 1990;28:394-403.
34. Wessels WJ, Marani E. A rostrocaudal somatotopic organization in the brachial dorsal root ganglia of neonatal rats. *Clin Neurol Neurosurg* 1993;suppl 95:S3-S11.
35. Prats-Galino A, Puigdemilliv-Sanchez A, Ruano-Gil D, et al. Representations of hindlimb digits in rat dorsal root ganglia. *J Comp Neurol* 1999;408:137-145.
36. Peyronnard JM, Charron LF, Lavoie J, et al. Motor, sympathetic and sensory innervation of rat skeletal muscles. *Brain Res* 1986;373:288-302.
37. Peyronnard JM, Messier JP, Dubreuil M, et al. Three-dimensional computer-aided analysis of the intraganglionic topography of primary muscle afferent neurons in the rat. *Anat Rec* 1990;227:405-417.
38. Henneman E, Somjen G, Carpenter DO. Functional significance of cell size in spinal motoneurons. *J Neurophysiol* 1965;28:560-580.
39. Ulfhake B, Cullheim S. A quantitative light microscopic study of the dendrites of cat spinal  $\gamma$ -motoneurons after intracellular staining with horseradish peroxidase. *J Comp Neurol* 1981;202:585-596.
40. Ishihara A, Hayashi S, Roy RR, et al. Mitochondrial density of ventral horn neurons in the rat spinal cord. *Acta Anat (Basel)* 1997;160:248-253.
41. Pannese E, Procacci P, Ledda M, et al. Age-related reduction of the satellite cell sheath around spinal ganglion neurons in the rabbit. *J Neurocytol* 1996;25:137-146.
42. Lawson SN, Crepps BA, Perl ER. Relationship of substance P to afferent characteristics of dorsal root ganglion neurones in guinea-pig. *J Physiol* 1997;505:177-191.
43. Costa M, Furness JB, Llewellyn-Smith IJ, et al. Projections of substance P-containing neurons within the guinea-pig small intestine. *Neuroscience* 1981;6:411-424.
44. Matteoli M, Haimann C, De Camilli P. Substance P-like immunoreactivity at the frog neuromuscular junction. *Neuroscience* 1990;37:271-275.
45. Fontaine B, Klarsfeld A, Hokfelt T, et al. Calcitonin gene-related peptide, a peptide present in spinal cord motoneurons, increases the number of acetylcholine receptors in primary cultures of chick embryo myotubes. *Neurosci Lett* 1986;71:59-65.
46. Johnson H, Hökfelt T, Ulfhake B. Galanin- and CGRP-like immunoreactivity coexist in rat spinal motoneurons. *Neuroreport* 1992;3:303-306.
47. Cortes R, Arvidsson U, Schalling M, et al. In situ hybridization studies on mRNAs for cholecystokinin, calcitonin gene-related peptide and choline acetyltransferase in the lower brain stem, spinal cord and dorsal root ganglia of rat and guinea pig with special reference to motoneurons. *J Chem Neuroanat* 1990;3:467-485.
48. Rodrigo J, Polak JM, Terenghi G, et al. Calcitonin gene-related peptide (CGRP)-immunoreactive sensory and motor nerves of the mammalian palate. *Histochemistry* 1985;82:67-74.
49. Gibson SJ, Polak JM, Giaid A, et al. Calcitonin gene-related peptide messenger RNA is expressed in sensory neurones of the dorsal root ganglia and also in spinal motoneurons in man and rat. *Neurosci Lett* 1988;91:283-288.
50. Pielh F, Arvidsson U, Hokfelt T, et al. Calcitonin gene-related peptide-like immunoreactivity in motoneuron pools innervating different hind limb muscles in the rat. *Exp Brain Res* 1993;96:291-303.
51. Forsgren S, Bergh A, Carlsson E, et al. Calcitonin gene-related peptide expression at endplates of different fibre types in muscles in rat hind limbs. *Cell Tissue Res* 1993;274:439-446.
52. Homonko DA, Theriault E. Downhill running preferentially increases CGRP in fast glycolytic muscle fibers. *J Appl Physiol* 2000;89:1928-1936.
53. Shi G, Tan H, Wan X, et al. Studies on distribution patterns of modulator CGRP in different motoneuron pools in rats [Chinese]. *Zhongguo Yi Xue Ke Xue Yuan Xue Bao* 1996;18:401-406.
54. Dietz V, Ketelsen U-P, Berger W, et al. Motor unit involvement in spastic paresis. Relationship between leg muscle activation and histochemistry. *J Neurol Sci* 1986;75:89-103.
55. Arvidsson U, Cullheim S, Ulfhake B, et al. Altered levels of calcitonin gene-related peptide (CGRP)-like immunoreactivity of cat lumbar motoneurons after chronic spinal cord transection. *Brain Res* 1989;489:387-391.
56. Sheehan G. The pathophysiology of spasticity. *Eur J Neurol* 2002;9(suppl 1):3-9.
57. Keith JR. Spastic paresis in beef and dairy cattle. *Vet Med Small Anim Clin* 1981;76:1043-1047.
58. Oku R, Satoh M, Fujii N, et al. Calcitonin gene-related peptide promotes mechanical nociception by potentiating release of substance P from the spinal dorsal horn in rats. *Brain Res* 1987;403:350-354.
59. Gamse R, Saria A. Potentiation of tachykinin-induced plasma protein extravasation by calcitonin gene-related peptide. *Eur J Pharmacol* 1985;114:61-66.
60. Brain SD, Williams TJ. Interactions between the tachykinins and calcitonin gene-related peptide lead to the modulation of oedema formation and blood flow in rat skin. *Br J Pharmacol* 1989;97:77-82.
61. Brain SD, Cambridge H, Hughes SR, et al. Evidence that calcitonin gene-related peptide contributes to inflammation in the skin and joint. *Ann N Y Acad Sci* 1992;657:412-419.
62. McCarthy PW, Lawson SN. Cell type and conduction velocity of rat primary sensory neurons with calcitonin gene-related peptide-like immunoreactivity. *Neuroscience* 1990;34:623-632.
63. Lawson SN, Crepps B, Perl ER. Calcitonin gene-related peptide immunoreactivity and afferent receptive properties of dorsal root ganglion neurones in guinea-pigs. *J Physiol* 2002;540:989-1002.
64. Hoheisel U, Mense S, Scheretzke R. Calcitonin gene-related peptide-immunoreactivity in functionally identified primary afferent neurones in the rat. *Anat Embryol (Berl)* 1994;189:41-49.
65. Ch'ng JL, Christofides ND, Anand P, et al. Distribution of

galanin immunoreactivity in the central nervous system and the responses of galanin-containing neuronal pathways to injury. *Neuroscience* 1985;16:343–354.

66. Moore RY. Cranial motor neurons contain either galanin- or calcitonin gene-related peptide-like immunoreactivity. *J Comp Neurol* 1989;282:512–522.

67. Wiesenfeld-Hallin Z, Xu XJ. Galanin in somatosensory function. *Ann N Y Acad Sci* 1998;863:383–389.

68. Ma W, Bisby MA. Differential expression of galanin immunoreactivities in the primary sensory neurons following partial and complete sciatic nerve injuries. *Neuroscience* 1997;79:1183–1195.

69. Mullen RJ, Buck CR, Smith AM. NeuN, a neuronal specific nuclear protein in vertebrates. *Development* 1992;116:201–211.

70. Chiocchetti R, Poole DP, Kimura H, et al. Evidence that two forms of choline acetyltransferase are differentially expressed in subclasses of enteric neurons. *Cell Tissue Res* 2003;311:11–22.